FOCUS ISSUE: SEMICONDUCTOR GAMMA CAMERA―REVIEW ARTICLE

Emerging Myocardial SPECT with ^{201}Tl Using Semiconductor Detectors: Clinical Application to Stress Myocardial Perfusion Scintigraphy

Mamoru Nanasato MD, PhD[1)], Takanaga Niimi BSc[2)], Mitsuo Sugimoto[2)] and Toyoaki Murohara MD, PhD[3)]

Received: March 31, 2016/Revised manuscript received: June 1, 2016/Accepted: June 2, 2016

Abstract

Novel single photon emission computed tomography (D-SPECT) scanners with solid-state semiconductor detectors using cadmium zinc-telluride (CZT) have been clinically applied. D-SPECT is a second scanner in Japan in which CZT detectors offer higher sensitivity and better spatial resolution than conventional Anger cameras. Myocardial counts are important to assure image quality that might be improved due to the favorable physical performance of the CZT detectors. Different physical properties between CZT detectors and Anger cameras alter the quality of myocardial SPECT images. The image quality of ^{201}Tl-SPECT improved after introducing CZT detectors to achieve that of ^{99m}Tc. In addition, results from ECG-gated myocardial SPECT in clinical practice such as left ventricular volumes and ejection fraction were similar. These results could be applied to patients in the same way as those of conventional Anger cameras. However, reverse redistribution appears myocardial ^{201}Tl-SPECT images of apparently normal persons. Uptake in apical areas is sometimes reduced. In conclusion, myocardial perfusion scintigraphy with ^{201}Tl and CZT detectors has been clinically applied in Japan. Some ^{201}Tl data from gamma cameras and CZT detectors are identical, but others differ. Further investigation is needed to optimize myocardial perfusion scintigraphy with ^{201}Tl.

Keywords: Cadmium zinc telluride, Image quality, Ischemic heart disease

Ann Nucl Cardiol 2016；2（1）：131-135

See page 122

Novel single photon emission computed tomography (SPECT) scanners with solid-state semiconductor detectors using cadmium zinc-telluride (CZT) have been applied in clinical practice. The D-SPECT scanner (Spectrum-Dynamics, Caesarea, Israel) is a second one that is available in Japan. It has nine square-hole tungsten collimators with vertically mounted CZT detector columns in 90° geometry. Each column comprises 1,024 (16×64), 5-mm-thick CZT elements (2.46×2.46 mm). Although the gamma camera appears fixed in front of a patient, data are acquired by synchronous rotation of these columns.

The sensitivity is better and spatial resolution is higher for CZT detectors than conventional Anger cameras (1, 2). Differences in the physical properties between the two cause variations in myocardial SPECT features. However, CZT detectors decrease the duration of examinations, reduce radiation exposure (3-5) and improve image quality (6). These detectors have been introduced mainly in the USA and Europe. Although the applicability of CZT detectors to myocardial SPECT with ^{99m}Tc has been investigated (1, 4, 7-12), little is known about their application to myocardial SPECT with ^{201}Tl. This article describes early experience myocardial D-SPECT with ^{201}Tl.

doi：10.17996/ANC.02.01.131

1) Mamoru Nanasato
Cardiovascular Center, Nagoya Daini Red Cross Hospital, 2-9 Myoken-cho, Showa, Nagoya, Aichi, Japan 466-8650
E-mail: nana@nagoya2.jrc.or.jp
2) Takanaga Niimi, Mitsuo Sugimoto
Department of Radiological Technology, Nagoya Daini Red Cross Hospital, Nagoya, Aichi, Japan
3) Toyoaki Murohara
Department of Cardiology, Nagoya University School of Medicine, Nagoya, Aichi, Japan.

Table 1 Comparison of patient characteristics on images generated by myocardial SPECT with ^{201}Tl and conventional Anger camera and, D-SPECT with ^{201}Tl and ^{99m}Tc

Variable	^{201}Tl-A-SPECT (n=609)	^{201}Tl-D-SPECT (n=581)	^{99m}Tc-D-SPECT (n=193)
Sex (male)	418 (68.6%)	424 (73.4%)	128 (66.3%)
Age (years)	69.8 ± 10.3	69.4 ± 10.6	67.2 ± 13.3
Height (cm)	161.0 ± 8.9	161.7 ± 12.9	160.3 ± 14.9
Weight (kg)	61.7 ± 12.1	62.0 ± 12.6	60.5 ± 13.5
Body mass index	23.7 ± 3.6	23.4 ± 3.7	23.1 ± 4.0
Stress test (exercise)	98/609 (16.0%)	76/581 (13.1%)	26/193 (13.5%)
Prior myocardial infarction	116/609 (19.0%)	116/581 (20.0%)	31/193 (16.1%)
Congestive heart failure	34/609 (5.6%)	40/508 (7.9%)	8/193 (4.1%)

A-SPECT: conventional Anger camera; D-SPECT: CZT detectors.

Acquisition protocol using CZT detectors (D-SPECT) and Anger camera (A-SPECT)

Stress and rest images were acquired using A-SPECT followed by D-SPECT from patients at 5 to 10 minutes and four hours, respectively, after intravenously injecting patients with 74-111 MBq of ^{201}Tl, or at 30 to 60 minutes after an intravenous injection of 300 to 600 MBq of ^{99m}Tc-tetrofosmin.

Image acquisition proceeded with the patients lying supine with both arms raised, and in a semi-reclining position with the left arm resting on top of the camera. A 30-second pre-scan before acquisition identified the location of the heart and set the angle limits of scanning for each detector, enabling scans of regions of interest. Stress and rest images were acquired over a period of six minutes. Images were gated at eight frames on ^{201}Tl and sixteen on ^{99m}Tc per cardiac cycle using an R-wave trigger and an acceptance window at 20% of the mean R-wave interval. Attenuation and scatter correction were not applied.

The conventional Anger camera (Millennium, GE, Hino, Japan) comprising a sodium iodide scintillation crystal and an L-shaped, dual-detector equipped with low-energy, multi-purpose collimators, was rotated in a 90° arc in a circular orbit from the 45° right anterior oblique to the 45° left posterior oblique positions in 32 increments of 20 seconds on ^{201}Tl or 30 seconds on ^{99m}Tc. The energy discriminator of the camera was set at a 70-keV photopeak for ^{201}Tl with a 20% window and a 140 keV photopeak for ^{99m}Tc with a 20% window. Filtered back-projection proceeded through a Butterworth filter. ECG-gating, attenuation and scatter correction were applied in the same manner to all images.

Image analysis

Image quality was visually scored using a four-point scale comprising excellent, good, fair and poor. Uptake on non-gated SPECT images was visually graded in all myocardial SPECT segments by the consensus of two observers who were unaware of previous findings. Excellent images are without background and extracardiac activity and thus suitable for diagnosis. Good images are sufficient for evaluating a diagnosis. Fair images can be evaluated, but accumulation on the myocardium is inhomogeneous. Poor images are unsuitable for clinical diagnosis because of features such as low myocardial counts, high background activity and extracardiac accumulation (13). Scores of 0, 1, 2, 3 and 4 on 17 segments of the left ventricle (14) indicate findings as normal, mildly, moderately and severely reduced, and absent, respectively. Summed stress scores (SSS) and summed rest scores (SRS) are defined as the total defect score for each myocardial SPECT stress and rest image. The summed difference score (SDS) is defined as SSS minus SRS.

Comparison of image quality between D-SPECT with ^{201}Tl and ^{99m}Tc and A-SPECT with ^{201}Tl

The quality was compared between stress/rest images acquired using conventional myocardial ^{201}Tl and ^{99m}Tc SPECT with CZT detectors in consecutive patients (n=588 and n=193, respectively) between May 2014 and January 2015. Another 609 patients were assessed by myocardial SPECT with ^{201}Tl and an Anger camera between May 2013 and April 2014. The patients' characteristics were similar among the three groups (Table 1). Fig. 1a shows representative findings of ischemia on myocardial SPECT images. The quality of the images acquired from myocardial D-SPECT with ^{201}Tl and ^{99m}Tc was similar (Fig. 2a) and significantly improved; 28.2%, 64. 1%, 6. 4% and 1. 4% were excellent, good and fair, respectively, compared with 15.4%, 54.7%, 27.0% and 2.9%, respectively, acquired by myocardial A-SPECT (Fig. 2b). The CZT detectors improved image quality with ^{201}Tl through reducing the number of fair-quality images from 27.0% to 6. 4%, during a shorter acquisition time (6 vs. 10 minutes 40 seconds). Another study found that myocardial D-SPECT with ^{201}Tl improved image quality compared with A-SPECT (15). This is an inevitable consequence of the physical properties of CZT detectors.

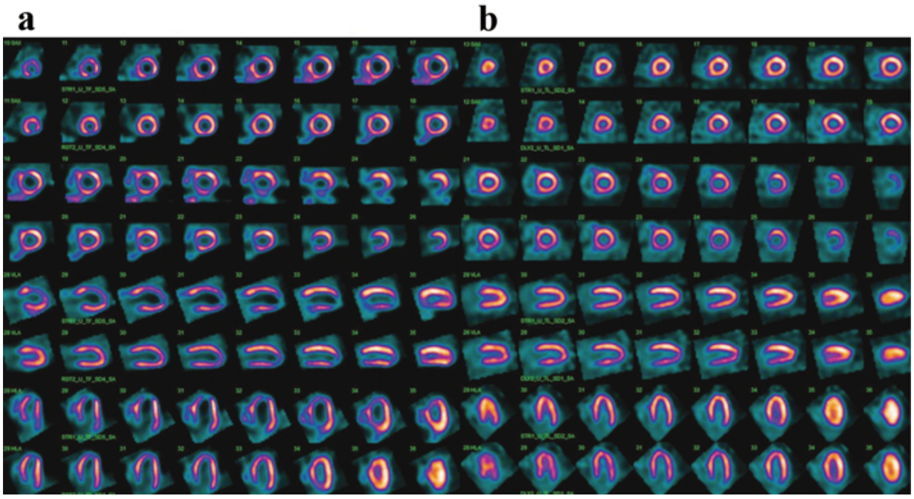

Fig. 1 Representative myocardial SPECT images of patients with myocardial ischemia and normal perfusion

a. Coronary angiograms of patient with myocardial ischemia show triple-vessel disease. Upper and lower rows are stress and rest, respectively.

b. Coronary angiograms of patient with normal perfusion show no significant stenosis. Upper and lower rows are stress and rest, respectively.

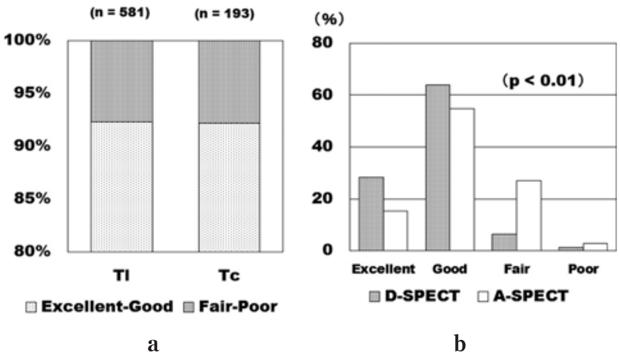

Fig. 2 Comparison of image quality on myocardial SPECT with ^{201}Tl

a. Proportions of various levels of image quality acquired using D-SPECT with ^{99m}Tc.

b. Comparison of image quality between A-SPECT (conventional Anger camera) and D-SPECT (CZT detectors). * Patients in supine position.

Application for ECG-gated myocardial SPECT

The applicability of ECG-gated myocardial A-SPECT with ^{201}Tl has been described (16-18). Data have been compared between images from supine patients acquired using CZT detectors and Anger cameras. One study found that quantitative ECG-gated myocardial D-SPECT with ^{99m}Tc correlated with data acquired A-SPECT (19), although the SPECT protocols differed between them. However, whether data acquired by ECG-gated myocardial D-SPECT and A-SPECT with ^{201}Tl are comparable has remained unclear.

Twenty-two patients with known or suspected angina pectoris underwent essentially simultaneous ^{201}Tl stress/rest ECG-gated myocardial D-SPECT and an A-SPECT because ^{201}Tl myocardial D-SPECT images were also acquired at rest from supine patients. We used an optimized version of Quantitative Gated SPECT software (Cedars AutoQuant; Cedars-Sinai, Los Angeles, CA, USA) to calculate end diastolic volume (EDV), end systolic volume (ESV) and ejection fraction (EF) on ECG-gated myocardial SPECT rest images.

Patients (twelve male; mean age was 67.6 ± 12.1 years; body mass index, 24.2 ± 4.1) were administered with 98.4 ± 22.2 MBq ^{201}Tl. The SSS, SRS and SDS were 1.6 ± 2.4, 1.7 ± 1.8 and -0.1 ± 1.9, respectively, on myocardial D-SPECT images and 2.0 ± 2.1, 1.6 ± 1.9, 0.4 ± 2.0, respectively, on those acquired using A-SPECT. Mean EDV, ESV, and EF were 70.1 ± 35.6 mL, 29.2 ± 26.5 mL and 63.0 ± 12.3%, respectively, on myocardial D-SPECT images and 67.9 ± 33.6 mL, 27.8 ± 27.5 mL and 65.0 ± 15.3%, respectively, on those acquired with A-SPECT (Fig. 3). Linear regression analyses of EDV, ESV and EF compared between ECG-gated myocardial D-SPECT and A-SPECT closely correlated (coefficients of r=0.987, 0.992 and 0.867, respectively; Fig. 3). Left ventricular function determined from D-SPECT and A-SPECT images were similar in clinical practice, although the images appeared quite different. The software algorithm is not fully open and this might explain the identical left ventricular volumes calculated by the software. The thresholds of ECG-gated myocardial D-SPECT and A-SPECT to determine the endocardial surface might be similar, as projection images from both are comparable. These results confirmed that quantitative analyses of data acquired by ECG-gated myocardial D-SPECT and A-SPECT are clinically applicable.

Normal images on the CZT detectors

Stress/rest myocardial D-SPECT with ^{201}Tl sometimes

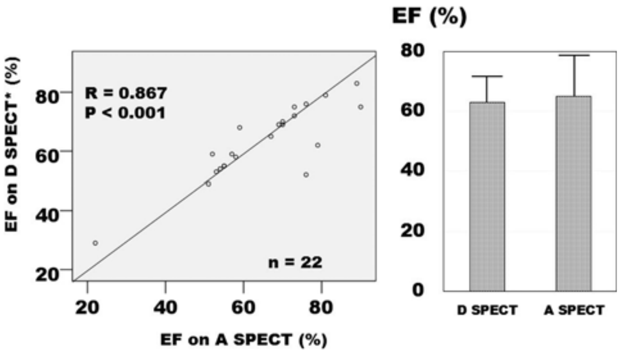

Fig. 3 Comparison of left ventricular ejection fraction determined by ECG-gated myocardial D-SPECT and A-SPECT with ^{201}Tl
Left column: results of linear regression analysis. Right column, mean difference in EF. A-SPECT: with conventional Anger camera; D-SPECT: with CZT detectors; EF: ejection fraction.

shows reduced uptake at the apex and/or apical inferior wall, resulting in emphasized ischemia in the apical area. Fig. 1b shows a representative image of normal perfusion acquired using myocardial SPECT. Data acquired from patients at low risk of ischemic heart disease according to their clinical background and normal findings on myocardial A-SPECT and D-SPECT with ^{201}Tl were analysed. The patients were classified as being at low risk when ECG abnormalities, structural heart disease, diabetes mellitus requiring medication, chronic kidney disease (estimated glomerular filtration rate <45 mL/min/1.73^2) and left ventricular asynergy (LVEF >50%) were absent. Normal images were defined as having SSS <2 without redistribution. Seventy of 840 patients were confirmed as being free of ischemia according to their clinical background and the findings of myocardial perfusion D-SPECT between May 2014 and May 2015. Stress/rest myocardial D-SPECT with ^{201}Tl revealed reverse redistribution in eight of the 70 patients and two had reverse redistribution in two consecutive areas, namely the apex and apical inferior wall. Six patients had reverse redistribution in the apical area. What reverse redistribution on stress/rest myocardial SPECT with ^{201}Tl actually means has remained controversial. Previous studies have found that reverse redistribution indicates a viable myocardium in patients with myocardial infarction, especially after receiving reperfusion therapy (20-22). Most of the reverse redistribution on stress/rest myocardial ^{201}Tl-SPECT in normal populations does not show as stenosis on coronary angiography or as a damaged myocardium.

The workstation for D-SPECT includes a normal file of North Americans who have been assessed by SPECT using ^{99m}Tc. However, physical properties differ between North Americans and Japanese (23-25). Previous studies have shown the relevance of a Japanese normal database to diagnose coronary artery disease and to assess prognoses among Japanese patients (26,27). A normal file of ^{201}Tl with CZT detectors should be established to improve the diagnosis of coronary artery disease using stress/rest myocardial SPECT.

Future perspectives and conclusions

Global hypoperfusion might be underestimated, because myocardial SPECT allows visualization of spatially relative perfusion abnormalities. Abnormalities in segments adjoining those that are clearly under-perfused are also difficult to evaluate. Several studies have established the diagnostic accuracy of applying washout rates on myocardial perfusion scintigraphy with ^{201}Tl to planar and myocardial SPECT images. This is especially important for patients with balanced ischemia and with minimally reduced uptake on myocardial SPECT. Washout rates are semi-automatically calculated by the software integrated into conventional Anger cameras (28, 29). The CZT detectors do not include software to calculate washout rates on images acquired by myocardial perfusion scintigraphy with ^{201}Tl. Such software should be developed to improve diagnostic accuracy.

Myocardial perfusion scintigraphy using CZT detectors and ^{201}Tl has been clinically applied in Japan. Some images differ between ^{201}Tl with CZT detectors and conventional Anger cameras. Further investigation is required to optimize myocardial perfusion scintigraphy with ^{201}Tl.

Acknowledgments

None

Sources of funding

None

Conflicts of interest

None to declare.

Reprint requests and correspondence:
Mamoru Nanasato, MD, PhD
Cardiovascular Center, Nagoya Daini Red Cross Hospital,
2-9 Myoken-cho, Showa, Nagoya, Aichi, Japan 466-8650
E-mail: nana@nagoya2.jrc.or.jp

References

1. Gambhir SS, Berman DS, Ziffer J, et al. A novel high-sensitivity rapid-acquisition single-photon cardiac imaging camera. J Nucl Med 2009; 50: 635-43.
2. Miyagawa M, Nishiyama Y, Tashiro R, et al. Novel cardiac SPECT technology with semiconductor detectors: Emerging trends and future perspective. Ann Nucl Cardiol 2015; 1 (1): 18-26.
3. Kudo T, Ideguchi R. The effects of medical radiation: A few things nuclear cardiologists must know. Ann Nucl Cardiol 2015; 1 (1): 35-42.

4. Nakazato R, Berman DS, Hayes SW, et al. Myocardial perfusion imaging with a solid-state camera: simulation of a very low dose imaging protocol. J Nucl Med 2013; 54: 373-9.
5. Einstein AJ, Pascual TN, Mercuri M, et al. Current worldwide nuclear cardiology practices and radiation exposure: results from the 65 country IAEA Nuclear Cardiology Protocols Cross-Sectional Study (INCAPS). Eur Heart J 2015; 36: 1689-96.
6. Einstein AJ, Blankstein R, Andrews H, et al. Comparison of image quality, myocardial perfusion, and left ventricular function between standard imaging and single-injection ultra-low-dose imaging using a high-efficiency SPECT camera: the MILLISIEVERT study. J Nucl Med 2014; 55: 1430-7.
7. Allie R, Hutton BF, Prvulovich E, et al. Pitfalls and artifacts using the D-SPECT dedicated cardiac camera. J Nucl Cardiol 2016; 23: 301-10.
8. Ben-Haim S, Almukhailed O, Neill J, et al. Clinical value of supine and upright myocardial perfusion imaging in obese patients using the D-SPECT camera. J Nucl Cardiol 2014; 21: 478-85.
9. Ben-Haim S, Murthy VL, Breault C, et al. Quantification of Myocardial Perfusion Reserve Using Dynamic SPECT Imaging in Humans: A Feasibility Study. J Nucl Med 2013; 54: 873-9.
10. Berman DS, Kang X, Tamarappoo B, et al. Stress thallium-201/rest technetium-99m sequential dual isotope high-speed myocardial perfusion imaging. JACC Cardiovascular imaging 2009; 2: 273-82.
11. Ko T, Utanohara Y, Suzuki Y, et al. A preliminary feasibility study of simultaneous dual-isotope imaging with a solid-state dedicated cardiac camera for evaluating myocardial perfusion and fatty acid metabolism. Heart Vessels 2016; 31: 38-45.
12. Nakazato R, Berman DS, Gransar H, et al. Prognostic value of quantitative high-speed myocardial perfusion imaging. J Nucl Cardiol 2012; 19: 1113-23.
13. Giorgetti A, Rossi M, Stanislao M, et al. Feasibility and diagnostic accuracy of a gated SPECT early-imaging protocol: a multicenter study of the Myoview Imaging Optimization Group. J Nucl Med 2007; 48: 1670-5.
14. Cerqueira MD, Weissman NJ, Dilsizian V, et al. Standardized myocardial segmentation and nomenclature for tomographic imaging of the heart. A statement for healthcare professionals from the Cardiac Imaging Committee of the Council on Clinical Cardiology of the American Heart Association. J Nucl Cardiol 2002; 9: 240-5.
15. Songy B, Lussato D, Guernou M, et al. Comparison of myocardial perfusion imaging using thallium-201 between a new cadmium-zinc-telluride cardiac camera and a conventional SPECT camera. Clinical Nucl Med 2011; 36: 776-80.
16. Bacher-Stier C, Muller S, Pachinger O, et al. Thallium-201 gated single-photon emission tomography for the assessment of left ventricular ejection fraction and regional wall motion abnormalities in comparison with two-dimensional echocardiography. Eur J Nucl Med 1999; 26: 1533-40.
17. Manrique A, Koning R, Cribier A, et al. Effect of temporal sampling on evaluation of left ventricular ejection fraction by means of thallium-201 gated SPET: comparison of 16- and 8-interval gating, with reference to equilibrium radionuclide angiography. Eur J Nucl Med 2000; 27: 694-9.
18. Wright GA, McDade M, Keeble W, et al. Quantitative gated SPECT myocardial perfusion imaging with ^{201}Tl: an assessment of the limitations. Nucl Med Commun 2000; 21: 1147-51.
19. Sharir T, Slomka PJ, Hayes SW, et al. Multicenter trial of high-speed versus conventional single-photon emission computed tomography imaging: quantitative results of myocardial perfusion and left ventricular function. J Am Coll Cardiol 2010; 55: 1965-74.
20. Akutsu Y, Kodama Y, Nishimura H, et al. Contractile reserve, thallium-201 reverse redistribution and mismatch between perfusion and metabolism in reperfused infarct-related myocardium with delayed and incomplete functional recovery. Jap Heart J 2004; 45: 739-48.
21. Beygui F, Le Feuvre C, Maunoury C, et al. Coronary vasodilator reserve: a clue to the explanation of ^{201}Tl redistribution patterns early after successful primary stenting for acute myocardial infarction. J Am Coll Cardiol 2002; 40: 877-81.
22. Roelants VA, Vanoverschelde JL, Vander Borght TM, et al. Reverse redistribution on exercise-redistribution ^{201}Tl SPECT in chronic ischemic dysfunction: predictive of functional outcome after revascularization? J Nucl Med 2002; 43: 621-7.
23. Nakajima K. Normal values for nuclear cardiology: Japanese databases for myocardial perfusion, fatty acid and sympathetic imaging and left ventricular function. Ann Nucl Med 2010; 24: 125-35.
24. Nakajima K, Kumita S, Ishida Y, et al. Creation and characterization of Japanese standards for myocardial perfusion SPECT: database from the Japanese Society of Nuclear Medicine Working Group. Ann Nucl Med 2007; 21: 505-11.
25. Nakajima K, Okuda K, Kawano M, et al. The importance of population-specific normal database for quantification of myocardial ischemia: comparison between Japanese 360 and 180-degree databases and a US database. J Nucl Cardiol 2009; 16: 422-30.
26. Yoda S, Nakanishi K, Tano A, et al. Diagnostic value of automated quantification of nuclear cardiology in Japanese patients with single vessel coronary artery disease: comparison between Japanese and American normal databases. J Cardiol 2013; 62: 224-9.
27. Yoda S, Nakanishi K, Tano A, et al. Usefulness of automated assessment of nuclear cardiology for prediction of major cardiac events in Japanese patients with known or suspected coronary artery disease: comparison with conventional visual assessment in a large-scale prognostic study. J Cardiol 2014; 64: 395-400.
28. Takao Y, Murata H, Katoh K. Availability and limitations of thallium-201 myocardial SPECT quantitative analysis: assessment as daily routine procedure for ischemic heart disease. Ann Nucl Med 1991; 5: 11-8.
29. Teragawa H, Yamagata T, Kato M, et al. Assessment of the severity of coronary artery stenosis by the ratio of the regional washout rate determined by adenosine triphosphate stress Tl-201 SPECT. J Nucl Cardiol 1999; 6: 324-31.